*Proceedings of the Global Engineering, Science and Technology Conference 2012*
*28-29 December 2012, Dhaka, Bangladesh*

# Experimental and Numerical Investigation of Flow over a Cylinder at Reynolds Number $10^5$

Toukir Islam and S.M. Rakibul Hassan

*Flow past a stationary circular cylinder at $Re=10^5$ is studied numerically using Navier-Stokes equation and solved via finite volume method. Numerical observations are compared with experimental results and with research works of other researchers. Different flow phenomena such as flow separation, pressure distribution over the surface, drag, vortex shedding etc. are also studied at different boundary conditions. A brief comparison between the 2D and 3D numerical calculations as well as the nature of voticity distribution and effect of surface roughness are extensively studied.*

**Field of research:** Mechanical Engineering.

**Keywords:** Separation, Coefficient of drag, Relative surface roughness, Karman Vortex street.

## 1. Introduction

Owing to geometric simplicity and widespread applications in real life, the flow past a circular cylinder has been extensively studied. Despite its simple shape, the flow past a circular cylinder produces several flow features associated with more complex geometries. Theoretical flow over a cylinder is considered to be inviscous, incompressible and irrotational; known as 'Potential Flow' in which the reattachment of streamlines is considered to be complete and symmetrical to detachment at the upstream resulting in zero drag and lift force. In real life, zero lift force is quite acceptable, but there must be a force on the body towards the flow direction i.e. more or less, drag is present in case of flow over the body. There is presence of viscosity and the flow is neither incompressible nor irrotational. Avoidance of viscosity in early era of fluid dynamics led to a paradox called 'D'Alembert's paradox' that remained as mystery for about one and half centuries until Ludwig Prandtl suggested the presence of thin viscous boundary layer in 1904. The variation of flow phenomena can de described with respect to Reynolds number as the fluid flow exhibits similar behavior within a particular range of Reynolds number. The trend of behavioral change also follows the change of Reynolds number.

Toukir Islam and S.M. Rakibul Hassan, Department of Mechanical Engineering, Bangladesh University of Engineering and Technology (BUET).
Toukir Islam, Room # 4007, Titumir Hall, BUET, Dhaka 1000, toukir.buet07@gmail.com
S.M. Rakibul Hassan, 16/5 khilgaon Bagicha,Dhaka 1219, rakibulhassan21@gmail.com

## 2. Literature Review:

The flow phenomena for flow over the stationary cylinder of fixed dimension depend on the free stream velocity and other conditions such as flowing fluid density, surface roughness etc. Anderson (Anderson, 2010) described the rejoins of different flows with respect to bands of Reynolds number. For flow in the region of 0< Re<4, streamlines are reattached similar way as they were detached resulting in near balance of pressure at upstream and downstream, known as 'Stokes flow'. 4<Re<40 region exhibits separation and wakes symmetrical to the flow axis. Above Re=40, the flow becomes unstable; vortices which were in fixed position starts to shed alternately in a regular fashion resulting in 'Von Karman vortex street'. With increasing Re, the Karman vortex street becomes turbulent and begins to metamorphose into distinct wake. The laminar boundary layer on the cylinder separates from the surface on the forward face. In this region of $10^3$<Re<$3\times10^5$, the transition of boundary layer from laminar to turbulent occurs with subsequent reduction of drag coefficient. At a definite Re, the drag coefficient becomes minimum. This phenomenon is known as 'Drag Crisis' and the Re at which it occurs is known as critical Reynolds number, $Re_c$. Re higher than the $Re_c$ exhibits increase in $C_D$ as the wake becomes flatter at downstream that increases pressure drag.

## 3. Methodology:

### 3.1 Numerical Procedure:

Numerical flow simulation is performed by solving Navier-Stokes equations, which are formulation of mass, momentum and energy conservation laws. To predict turbulent flows, the Favre-averaged Navier-Stokes equations are used, where time averaged effects of the flow turbulence on the flow parameters are considered. The conservation laws for mass, angular momentum and energy in the Cartesian coordinate system rotating with angular velocity Ω about an axis passing through the coordinate system's origin can be written in the conservation form as follows (SolidWorks Flow Simulation, 2012):

$$\frac{\partial \rho}{\partial t} + \frac{\partial (\rho u_i)}{\partial x_i} = 0$$

$$\frac{\partial (\rho u_i)}{\partial t} + \frac{\partial (\rho u_i u_j)}{\partial x_j} + \frac{\partial \mathrm{P}}{\partial x_i} = \frac{\partial}{\partial x_i}\left(\tau_{ij} + {\tau_{ij}}^R\right) + S_i$$

$$\frac{\partial (\rho H)}{\partial t} + \frac{\partial (\rho u_i \mathrm{H})}{\partial x_i} = \frac{\partial}{\partial x_i}\left[u_j\left(\tau_{ij} + {\tau_{ij}}^R\right)\right] + \frac{\partial \rho}{\partial t} + S_i u_i - {\tau_{ij}}^R \frac{\partial u_i}{\partial x_i} + \rho\varepsilon$$

$$H = \frac{u^2}{2}$$

Here $u$ is fluid velocity, $\rho$ is fluid density, $S_i$ is a mass-distributed external force per unit mass due to porous media resistance , a buoyancy (- $\rho g_i$), and the coordinate system's

rotation, $\tau_{ij}$ is the viscous shear stress tensor, $\tau_{ij}{}^{R}$ is Reynolds-stress tensor. The subscripts are used to denote summation over the three coordinate directions. *k-ε* turbulence model is used for the turbulent kinetic energy and its' dissipation rate. No slip conditions and adiabatic wall conditions are applied. Computational domain of 22″×16″×13″ was used for calculation for cylinder of 3″ diameter. No heat generation or transfer is considered.

The cell-centered finite volume (FV) method is used to obtain conservative approximations of the governing equations on the locally refined rectangular mesh. The governing equations are integrated over a control volume which is a grid cell, and then approximated with the cell-centered values of the basic variables. The integral conservation laws may be represented in the form of the cell volume and surface integral equation:

$\frac{\partial}{\partial t}\int \mathbf{U}\,\mathrm{dv} + \oint F.ds = \int Qdv$ , which is replaced by $\frac{\partial}{\partial t}(U\mathrm{v}) + \sum_{cell\ faces} F.s = Qv$

The second-order upwind approximations of fluxes F are based on the implicitly treated modified Leonard's QUICK approximations (Roache, 1998) and the Total Variation Diminishing (TVD) method (Hirsch, 1988).

## 3.2 Experimental Procedure:

Fluid mechanics Lab facilities of Bangladesh University of Engineering and Technology (BUET) was used to study the flow over the cylinder experimentally. The set-up wind tunnel consists of two induced fans, adjusting damper to control flow, pitot tubes and pressure tapping arrangements for inclined manometer (manometric fluid is water). A hollow cylinder of 3 inch dia; placed across the wind tunnel was subjected to the flow which had a pressure tapping on its surface. The cylinder was rotated on its own axis and angle indicator on the face of the cylinder was used to indicate the position of the pressure tap; thus the rotation angle. Two pitot tubes were used; one on the upstream and another on the downstream of the flow. Each pitot tube had an adjacent pressure tap. Pitot tubes could be moved vertically to take reading at different vertical positions. Now if $h_m$ is manometric deflection and $\rho_m$, $\rho_a$ are the density of manometric fluid and air respectively, then the free stream velocity

$$V_\infty = \sqrt{\frac{2g\times\ hm\times \rho\mathrm{m}}{\rho\mathrm{a}}}$$

If we want the flow of a definite Reynolds number, we just have to set $h_m$ accordingly. Here $h_m = (h_2 - h_1)$. Now the difference between the free steam static pressure and the pressure on the surface of the cylinder is $(h_5 - h_1)$ and the free stream dynamic pressure is $(h_2 - h_1)$; we can defy Cp as

$$Cp = \frac{(h5 - h1)}{(\mathrm{h2} - \mathrm{h1})}$$

($h_2$ –$h_1$) remains constant for a Reynolds number and measured once. So, several readings of ($h_5$ – $h_1$) are taken by rotating the cylinder anti clockwise direction from 0° to 350°; 10° for each rotation. The coefficient of drag is measured by the area under the curve Cp vs sinθ.

Fig 1: Schematics of Experimental setup

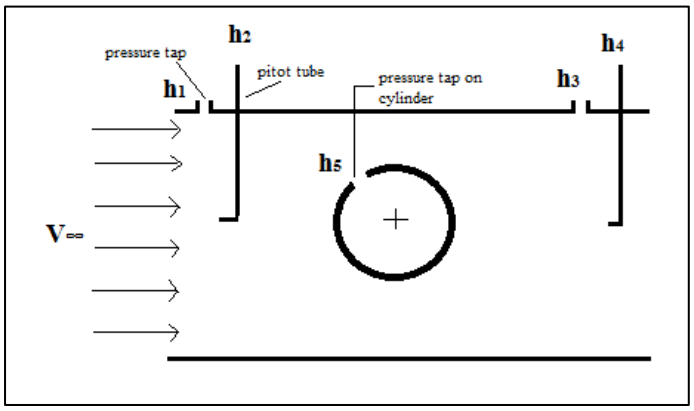


## 4. Results and discussions:

2D and 3D numerical calculations at zero roughness, 2D numerical calculations at various roughness and experimental calculation, all at Re=$10^5$ are done here. Fig 2 represents the variation of $C_P$ with respect to angular position θ of the stationary cylinder. Here θ is taken anti-clockwise direction from the upstream stagnation point. We know that, at the onset of separation, $C_P$ becomes unstable. The angle at which the separation occurs is known as separation angle. Separation angle on the upper and lower surface of the cylinder shoulder can de denoted as $\theta_{SU}$ and $\theta_{SL}$ respectively. The separation angles at different numerical and experimental calculations are presented in the table 1 and the observations are based on Fig 2. A secondary local suction peak on the surface of the cylinder at an angle around 315 degree for experimental $C_P$ is observed. Singh and Mittal (Singh, Mittal, 2005) observed similar suction peak at Re=$10^5$ and concluded that the peaks occur beyond the shoulder of the cylinder and points to the presence of a local recirculation zone close to the surface.

Fig 2: Distribution of $C_P$ at different angular position on the cylinder surface.

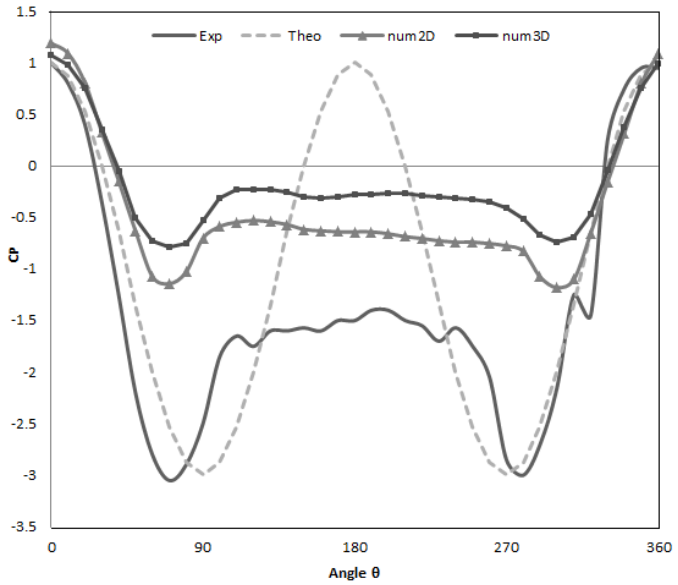


Table 1: Separation angle

| 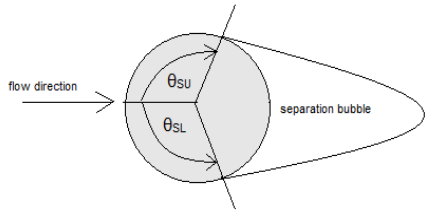  | Angle (in degree) | Numerical (Zero roughness) | | Experimental |
|---|---|---|---|---|
| | | 2D | 3D | |
| | $\theta_{SU}$ | 80 | 80 | 100 |
| | $\theta_{SL}$ | 90 | 100 | 100 |

We observe asymmetrical separation at upper and lower surfaces. Now the $C_D$ for 2D and 3D calculations for smooth surface is found to be 0.771 and 0.553 respectively. As we see, the $C_D$ for 2D calculation is bit over predicted. Mittal and Balachander (Mittal, Balachander, 1995) observed the similar results and concluded that the higher value of drag coefficient in 2D simulation is caused due to higher level of Reynolds stresses resulting in a shorter formation length behind the bluff body. Now $C_D$ for experimental results derived from the area under the curve $C_P$ Vs. sinθ (Fig 3) is 1.96. This result is well over-predicted compared to experimental result of Achenbach (Achenbach, 1968) which is around 1.06. Probable reason for the deviation is the difference in surface roughness. Fig 4 shows the change of $C_D$ at $Re=10^5$ with respect to different relative surface roughness for 2D numerical calculations. Relative surface roughness is the ratio of roughness to the diameter of the cylinder and denoted as $K_S/D$. For example, for roughness 300 micrometer of a cylinder of 0.0762 meter diameter, relative surface roughness will be 0.00394. From the figure, it is evident that, the $C_D$ decreases with

increasing $K_S/D$ up to a certain $K_S/D$; where it is minimum and after that, the $C_D$ increases with increasing roughness. The relative roughness at which the $C_D$ is minimum can be noted as critical roughness, $(K_S/D)_C$. Achenbach and Heinecke (Achenbach, Heinecke, 1981) suggested that the critical Reynolds number i.e. Reynolds number at which the $C_D$ becomes minimum for the flow over the cylinder at different Re; decreases with increasing surface roughness and the $C_D$ at the critical Reynolds number increases with increasing roughness.In case of 2D numerical calculation at Re $=10^5$, the $(K_S/D)_C$ is found to be 0.003937008 and $C_D$ at that point is around 0.43. Okajima and Nakamura (ADACHI, 1995) found $(K_S/D)_C$ to be 0.00468 and $C_D$ at that roughness is just above 0.5 for Re $10^5$.

Fig 3: $C_P$ Vs. sinθ at Re $10^5$ (experimental)

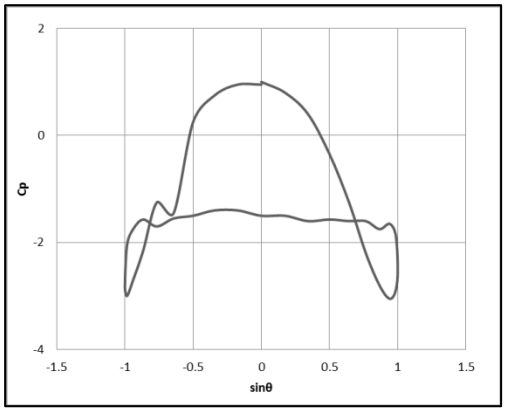


Fig 4: $C_D$ at different Ks/D

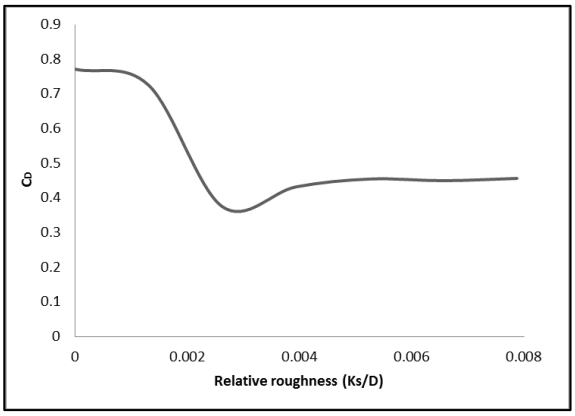


From the velocity contour representation (Fig 5(a),5(b)) for both 2D and 3D numerical calculations for smooth surface, the wake structures are visible but they are not as well organized and periodic as in Karman street at lower subcritical (Fig 5(c)) Reynolds number. Wakes are narrower resulting in much delayed separation. The unstable shear layer is much closer to the point of separation. Asymmetric vorticity distribution also observed from Fig 6 that results in variation of force towards axial direction (z direction).

Fig 5: Velocity contours (a) Re $10^5$, 2D simulation (b)Re $10^5$, 3D simulation (c)Re 67, 2D simulation

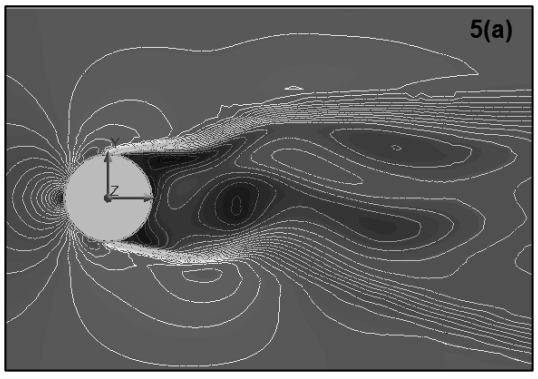


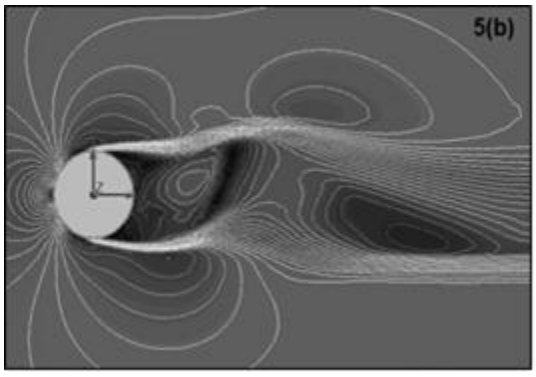

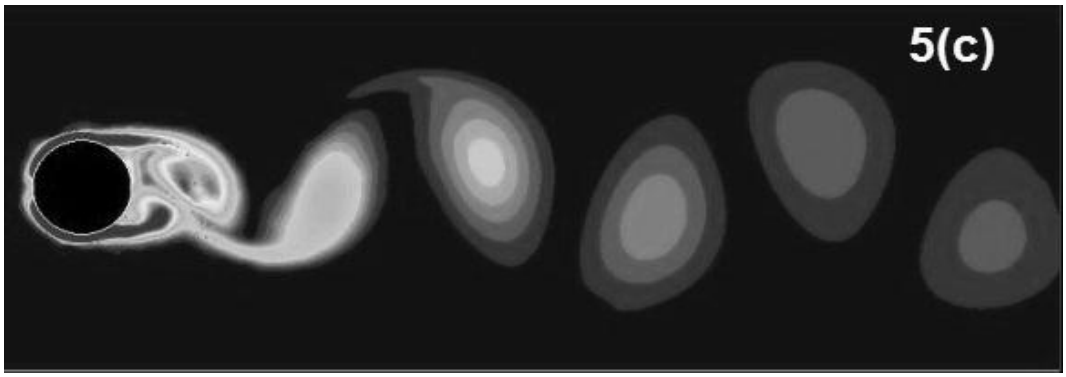


Fig 6: Vorticity distribution visible from the top view of the cylinder at (a) center plane, (b) 0.02 meter offset from center plane, (c) 0.04 meter offset from center plane.

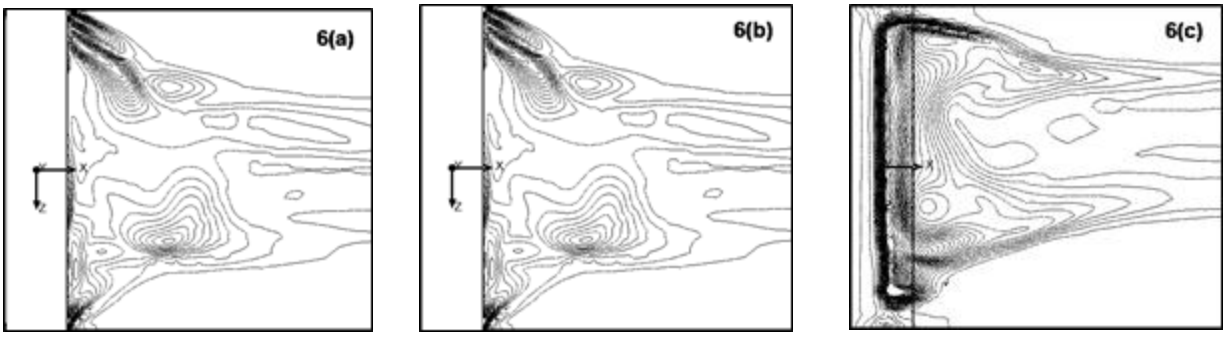


## 5. Conclusion:

Flow over the stationary cylinder is studied at a subcritical Re= $10^5$ through experiments and numerical calculations using finite volume method to solve Navier-Stokes equations. Though 2D numerical calculation is vital to predict drag crisis phenomena and shear layer instability, 3D numerical calculation provides us the overall idea about the real flow phenomena. Surface roughness and turbulence intensity controls the nature of the flow over a bluff body. In this article, the effect of surface roughness on drag coefficient and shift of critical Reynolds number due to relative roughness are illustrated through 2D numerical calculations. For a definite relative roughness, transition of boundary layer occurred at Re as low as $10^5$. Vorticity distribution in parallel and perpendicular to flow directions found to be asymmetrical that may cause vibration and lift or drag force.

## 6. References:


[1] Achenbach, E. 1968 Distribution of local pressure and skin friction around a circular cylinder in cross-flow up to Re = 5× 106. J.Fluid Mech. 34, 625-639.

[2] Achenbach,E. and Heinecke, E. On vortex shedding from smooth and rough cylinders in the range of Reynolds numbers 6 $\times 10^3$ to 5 $\times 10^6$. Journal of Fluid Mechanics, 109:239-251,1981.

[3] ADACHI,TSUTOMU. International Journal of Rotating Machinery,1995, Vol. 1, No. 3-4, pp. 187-197

[4] Anderson, John D.,Jr, Fundamental of Aerodynamics [In SI unit], Fifth Edition, NEW DELHI : Tata McGraw Hill Education Private Limited, 2010.

[5] Hirsch,C., 1988. Numerical computation of internal and external flows. John Wiley and Sons, Chichester.

[6] Mittal, R. and Balachander, S., Effect of three-dimensionality on the lift and drag of nominally two-dimensional cylinders. Physics of Fluids, 7:1841- 1865,1995.

[7] Roache,P.J.,1998,Technical Reference of Computational Fluid Dynamics, Hermosa Publishers, Albuquerque, New Mexico, USA.

[8] Singh, S.P. and Mittal, S., Flow Past a Cylinder: Shear Layer Instability and Drag Crisis, International Journal for Numerical Methods in Fluids, 47, 2005, 75—98.

[9] SolidWorks Flow Simulation 2012, Technical Reference.